JOURNAL OF GEOPHYSICAL RESEARCH, VOL. 108, NO. B9, 2442, doi:10.1029/2002JB001973, 2003

Three-dimensional velocity structure of crust and upper mantle in southwestern China and its tectonic implications

Chun-Yong Wang
Institute of Geophysics, China Seismological Bureau, Beijing, China

W. Winston Chan
Multimax, Inc., Largo, Maryland, USA

Walter D. Mooney
U.S. Geological Survey, Menlo Park, California, USA

Received 13 May 2002; revised 17 March 2003; accepted 29 April 2003; published 25 September 2003.

[1] Using P and S arrival times from 4625 local and regional earthquakes recorded at 174 seismic stations and associated geophysical investigations, this paper presents a three-dimensional crustal and upper mantle velocity structure of southwestern China (21°–34°N, 97°–105°E). Southwestern China lies in the transition zone between the uplifted Tibetan plateau to the west and the Yangtze continental platform to the east. In the upper crust a positive velocity anomaly exists in the Sichuan Basin, whereas a large-scale negative velocity anomaly exists in the western Sichuan Plateau, consistent with the upper crustal structure under the southern Tibetan plateau. The boundary between these two anomaly zones is the Longmen Shan Fault. The negative velocity anomalies at 50-km depth in the Tengchong volcanic area and the Panxi tectonic zone appear to be associated with temperature and composition variations in the upper mantle. The Red River Fault is the boundary between the positive and negative velocity anomalies at 50-km depth. The overall features of the crustal and the upper mantle structures in southwestern China are a low average velocity, large crustal thickness variations, the existence of a high-conductivity layer in the crust or/and upper mantle, and a high heat flow value. All these features are closely related to the collision between the Indian and the Asian plates. *INDEX TERMS:* 7205 Seismology: Continental crust (1242); 7218 Seismology: Lithosphere and upper mantle; 8123 Tectonophysics: Dynamics, seismotectonics; *KEYWORDS:* seismic tomography, regional earthquakes, 3-D velocity structure, Moho discontinuity, network method, plate collision

Citation: Wang, C.-Y., W. W. Chan, and W. D. Mooney, Three-dimensional velocity structure of crust and upper mantle in southwestern China and its tectonic implications, *J. Geophys. Res.*, *108*(B9), 2442, doi:10.1029/2002JB001973, 2003.

1. Introduction

[2] Southwestern China consists of the broad Yunnan and Sichuan Provinces where its tectonics has been closely related to the collision between the Indian and Asian plates since 45 Ma. Several lines of evidence indicate that the collision of the two plates strongly deformed the crust of southwestern China, and the deformation has continued up to the present. In addition, southwestern China lies in the southern segment of the South-North Seismic Zone of China where the seismic activity is very high. Since the 1970s, a series of large earthquakes with magnitude $M > 7.0$ have occurred in southwestern China, such as the 1970 Tonghai earthquake (M 7.7), the 1973 Luhou earthquake (M 7.6), the 1974 Zhaotong earthquake (M 7.1), the 1976 Longling earthquake (M 7.4), the 1976 Songpan earthquake (M 7.2), the 1988 Lancang-Genma earthquake (M 7.6), the 1995 China-Burma boundary earthquake (M 7.4), and the 1997 Lijiang earthquake (M 7.0). In addition, the Tengchong area in southwestern Yunnan is one of the presently active volcanic areas in China.

[3] Regional telemetric seismic networks established in Yunnan and Sichuan Provinces in early 1980s have been used to monitor the regional seismic activity, and have accumulated considerable amount of seismic data. The objective of this study, based on local and regional arrival time data recorded by the networks, is to develop a three-dimensional (3-D) crustal and upper mantle velocity structure beneath southwestern China, to elaborate the features of crustal and upper mantle structure in southwestern China affected by the collision between the Indian and Asian plates, and to discuss the deep environment where large earthquakes occur.

2. Regional Geologic Setting and Earlier Geophysical Studies

[4] Southwestern China is composed of six tectonic units [*Chen et al.*, 1987], as follows: the Bomi-Tengchong fold

0148-0227/03/2002JB001973$09.00

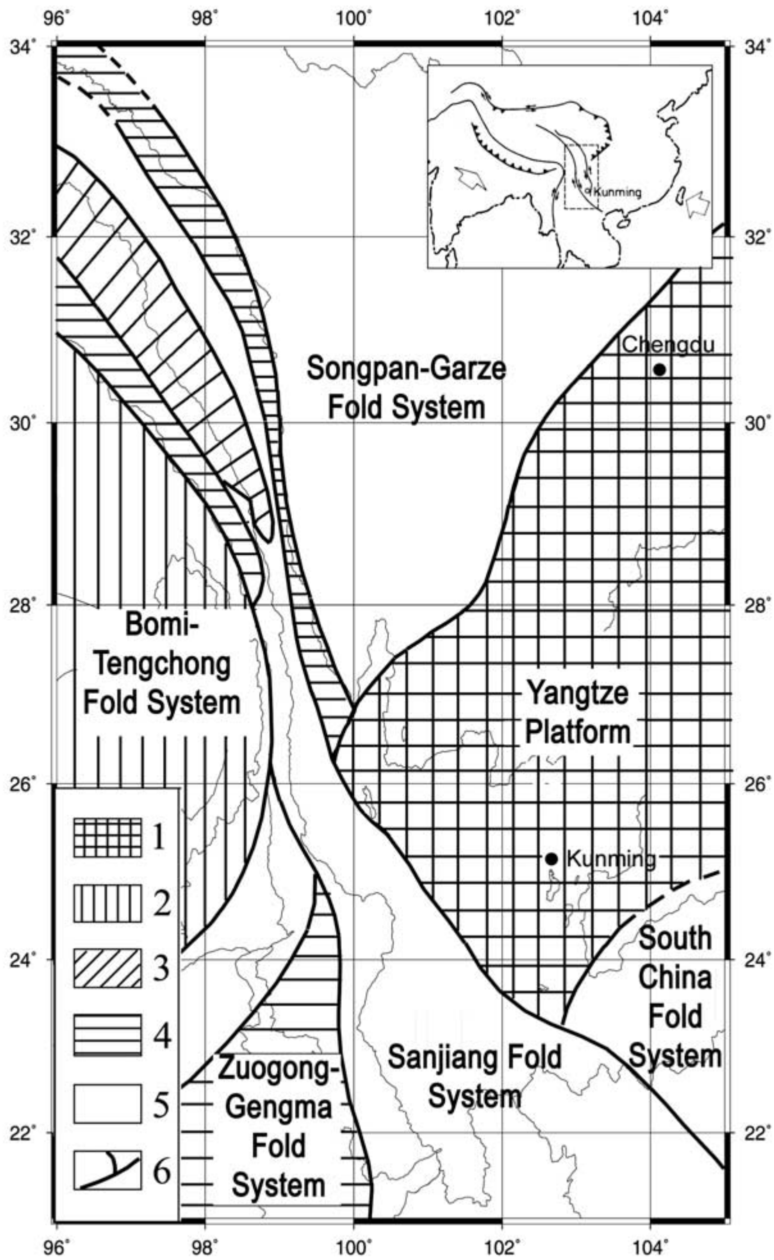

Figure 1. Schematic map of tectonics in southwestern China [modified from *Chen et al.*, 1987]: 1, platform; 2, early Caledonian fold zone; 3, late Caledonian fold zone; 4, Variscan fold zone; 5, Indo-China fold zone; 6, boundary between main tectonic units.

system, the Zuogong-Genma fold system, the Sanjiang fold system, the Songpan-Garze fold system, the Yangtze Platform and the South China fold system (Figure 1). The Longmenshan Fault Belt is considered as an important tectonic boundary, with Songpan-Garze Fold System to the west, and Yangtze Craton to the east. The Songpan-Garze fold system was a platform before Triassic, evolved into a fold zone during the latest episode of Indo-China movement, and then uplifted to land in Jurassic and Cretaceous. Slightly metamorphosed rocks of Paleozoic and Mesozoic in Songpan-Garze fold zone thrust over neritic and terrestrial sedimentary formation in Yangtze Platform [*Ren et al.*, 1980]. The Xianshuihe Fault belt is a left lateral strike-slip fault in Quaternary [*Allen et al.*, 1991] in the Songpan-Garze fold zone. Along this fault, many strong earthquakes have occurred during the last century. The Red River fault is the boundary between Sanjiang fold system and Yangtze Platform. On the basis of drainage dislocations, *Allen et al.* [1984] concluded that the Red River Fault had a dextral offset of 5.5 km in the Quaternary. *Tapponnier et al.* [1990], however, inferred that this fault was a plastic strike-slip shear fault in the Tertiary and its total left lateral shear dislocation is larger than 80 km. *Leloup et al.* [1995] suggested that the Ailaoshan-Red River belt exhibits a shear

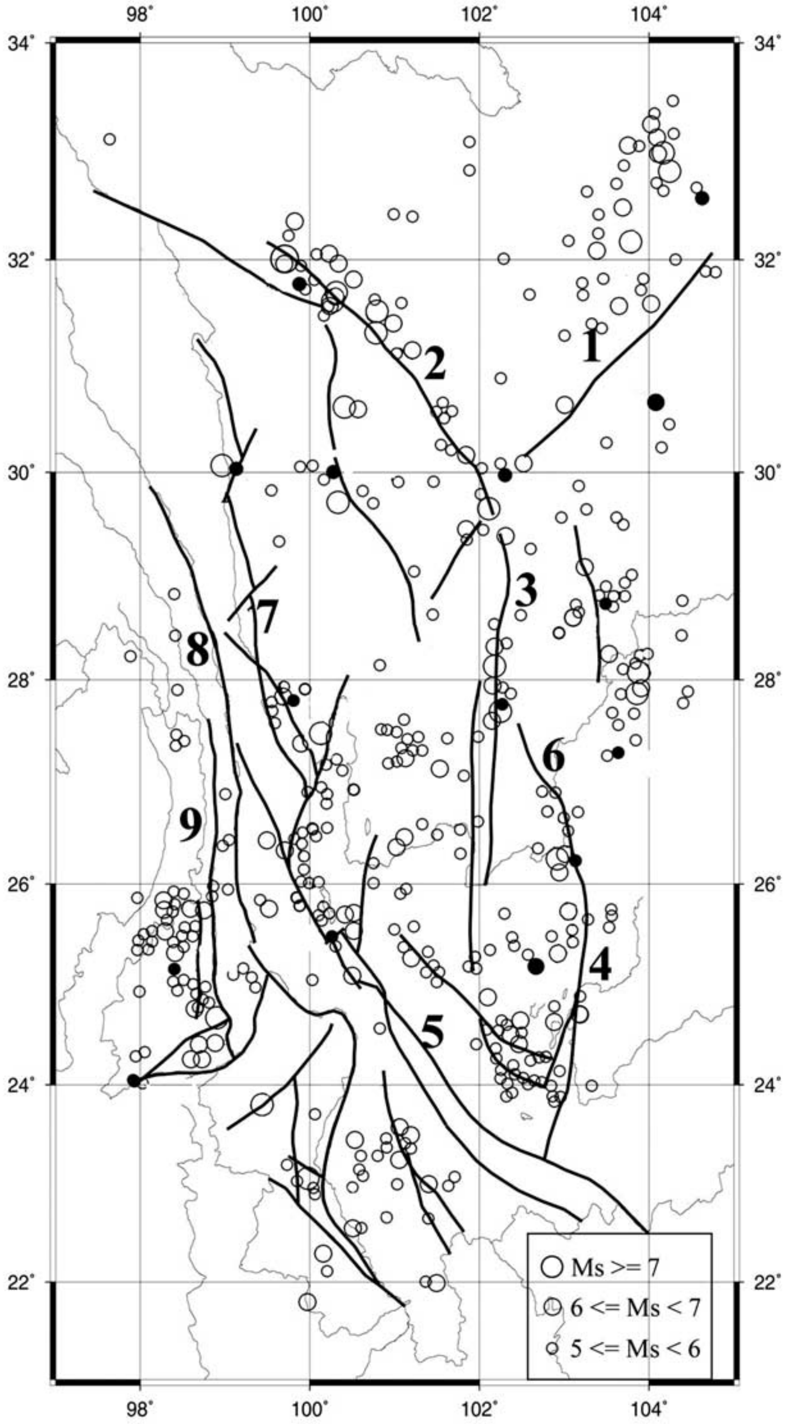

Figure 2. Location of major faults and epicenters of earthquakes with $M > 5.0$ in the study area: 1, Longmen Shan Fault; 2, Xianshuihe Fault; 3, Anninghe Fault; 4, Xiaojiang Fault; 5, Red River Fault; 6, Zemuhe Fault; 7, Jinshajiang Fault; 8, Lancangjiang Fault; 9 Nujiang Fault.

displacement as large as 700 km and is an ideal model of large-scale and high-temperature, strike-slip shear fault in the lower crust noted for its geological youth and strong deformation.

[5] The Sichuan-Yunnan Rhombic Block is bounded by several faults: the Anninghe Fault, Zemuhe Fault, Xiaojian Fault in the east, the Jinshajiang Fault and Red River Fault in the west, and the Xianshuihe Fault in the north (Figure 2). These boundary faults are thought of as channels for magma intrusion and volcanic eruption [*Li*, 1993].

[6] The Tengchong area in western Yunnan, belonging to the Bome-Tengchong fold system, is an active volcanic area in the Cenozoic Era. The focal mechanisms of shocks in the Tengchong and adjacent region show this area to be

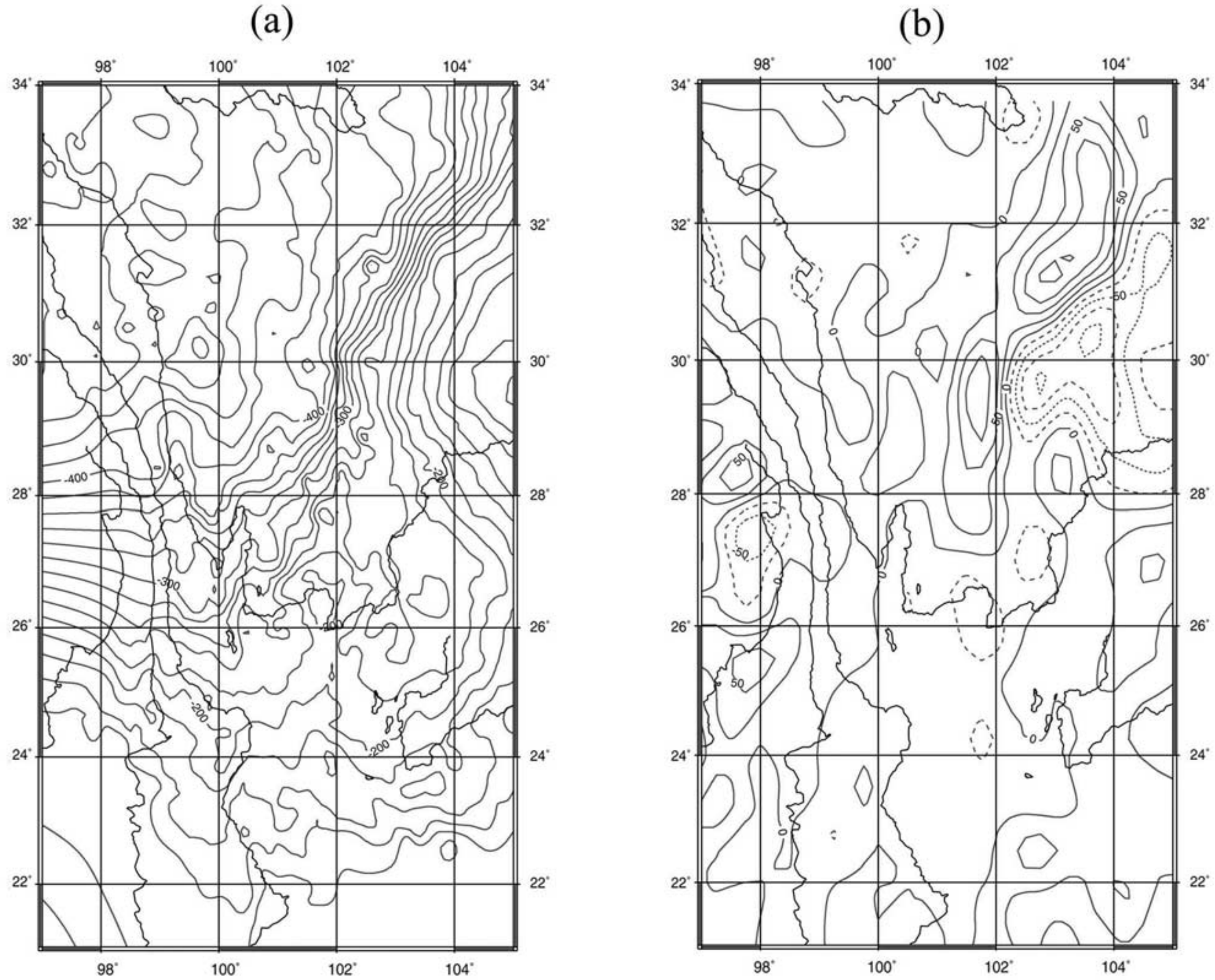

Figure 3. (a) Bouguer gravity anomaly (unit, mgal) and (b) free air anomaly maps, derived from the Bouguer anomaly in southwestern China.

dominated by the lateral compress-shear action exerted by the Burma intermediate-depth earthquake zone located in the eastern margin of the Indian plate [*Jiang*, 1985].

[7] Bouguer gravity anomalies in southwestern China (Figure 3a) decrease from -100 mgal in southeast to -450 mgal in northwest. A NNE trending gravity gradient belt, about 150 km wide and 900 km long, coincides with the Longmenshan Fault belt. In addition, there is also a NNW trending gravity gradient belt with gradient of about 1.1 mgal/km in the northwestern Yunnan [*Li*, 1993]. The residual anomalies of gravity show that the Red River Fault is located at the boundary between the positive and negative anomaly areas. The free-air anomaly map, derived from the Bouguer anomaly, is shown in Figure 3b.

[8] Over the last 20 years, several deep seismic sounding projects have been carried out in southwestern China (Figure 4). In Sichuan Province, the triangle profiles that traverse the Longmenshan Fault belt [*Chen et al.*, 1986] show the crustal thickness to increase from about 40 km in the Yangtze platform to 53 km in the Songpan-Garze fold zone. The Huashixia-Jianyang seismic profile shows that the mean crustal velocity in the Songpan-Garze fold zone is about 6.30 km/s, and the crustal thickness in the western Sichuan plateau is about 60 km [*Cui et al.*, 1996]. Along the Lijiang-Zhehai, Lijiang-Xinshizhen and Lazha-Changheba profiles, all of which traverse the Panxi tectonic zone, a low-velocity zone exists in the middle crust and uppermost mantle [*Xiong et al.*, 1986].

[9] In Yunnan Province, two deep seismic sounding experiments were carried out in 1982 and 1987, respectively, when six seismic profiles were completed [*Hu et al.*, 1986; *Kan et al.*, 1986; *Yan et al.*, 1985; *Lin et al.*, 1993]. The interpretation indicated that the crustal structure in the Yunnan area is laterally heterogeneous. The general trend of the Moho discontinuity becomes deeper from southeast to northwest. The Red River Fault belt is a main boundary of crustal structure in the Yunnan area, and in the southern segment of the fault, the depth of Moho increases from 38 km south of the fault to 43 km on the north side. In the northern segment of the fault, the Moho depth increases from 47 km to 56 km, and the mean crustal velocity is about 6.20 km/s north of the fault and about 6.40 km/s to the south. Moreover, on most seismic record sections, an intracrustal reflected phase Pc appears clearly, and the depth of related

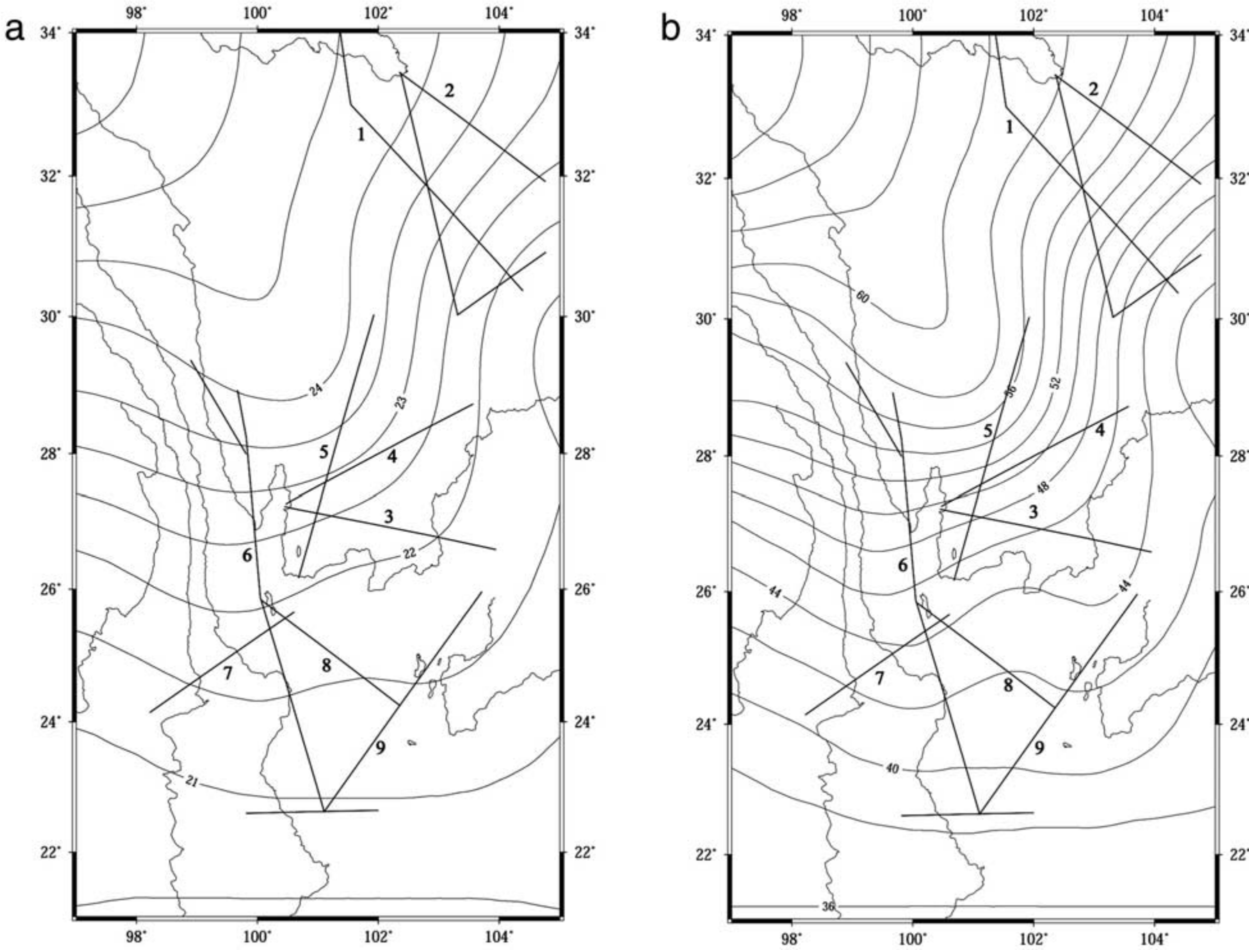

Figure 4. Depth isoline map of (a) Conrad discontinuity and (b) Moho discontinuity (unit, km), where the straight line marks deep seismic sounding profiles: 1, Huashixia-Jianyang profile; 2, Longmen Shan triangle profile; 3, Lijiang-Zhehai profile; 4, Lijiang-Xinshizhen profile; 5, Lazha-Changheba profile; 6, Zhongdian-Simao profile; 7, Zhefang-Binchuan profile; 8, Eryuan-Jiangcuan profile; and 9, Simao-Malong profile.

discontinuity is in the range of 20 km to 30 km. The depth of the Conrad and Moho discontinuities in southwestern China were obtained (Figures 4a and 4b) based on the velocity model obtained by deep seismic sounding profiles and the Bouguer gravity anomaly data (Figure 3a).

[10] Determination of the 3-D velocity structure in southwestern China using earthquake data has been performed several times [e.g., *Liu et al.*, 1989; *Chen et al.*, 1990, *Wang et al.*, 1994]. Because the seismic data sets they used were relatively small, or the topography of Moho was ignored, their results represent only a rough velocity structure, showing no details of velocity structure in the crust and upper mantle.

3. Inversion of 3-D Velocity Structure

3.1. Method

[11] The method for determining the 3-D crustal velocity structure beneath a seismic network, using regional *P* wave arrival time data, was first proposed by *Aki and Lee* [1976] and since then has been extensively modified. The benefit of using regional arrival time data is that the incident angle is variable within a large range and the result provides good resolution of the intracrust structure. The precondition of this technique is that the coupling between hypocenter parameters and velocity distribution has to be considered carefully. Among several techniques employed for travel time inversion, we selected a method based upon the LSQR algorithm and developed by *Zhao* [1991]. The advantage of Zhao's method is that it is able to consider velocity discontinuities of complicated shape in the crust and upper mantle. *Zhao et al.* [1992] developed a ray tracing method for calculating the travel time in 3-D medium. It works well in a lateral heterogeneous medium with complicated velocity discontinuities.

3.2. Seismic Data

[12] The regional seismic data we used here were collected from 174 seismic stations of the Yunnan and Sichuna networks (Figure 5). The basic data set includes about 6000 local

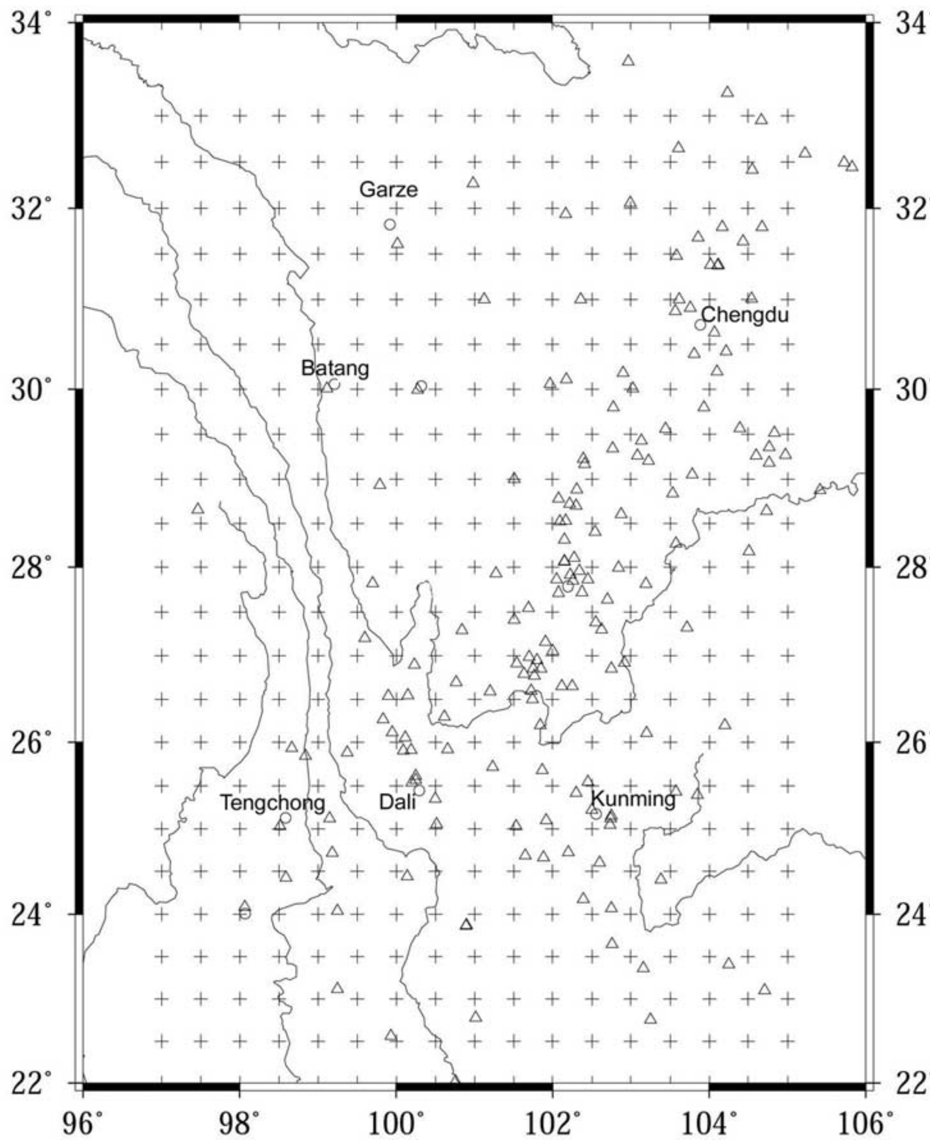

Figure 5. Location of seismic stations (triangles) and the grid nodes (crosses).

and regional earthquakes selected from catalogs for the period 1982–1999. Most earthquakes are of grade 1 or 2 of location precisions (i.e., location error less than 10 km), and a few are of grade 3 (location error less than 20 km). Among the 174 stations, some were in operation only for limited time periods. For the purpose of convergence in location processing, we adopted the following criteria for selecting events: The maximum azimuthal gap of station distribution is not larger than 160°, the minimum number of *P* wave arrival times is 8, and the maximum travel time residual is 3.0 s.

[13] After data selection, the number of events involved in the inversion is reduced to 4625 (Figure 6), and the total number of the observations is 112240, out of which 65170 are for *P* waves and 47120 for *S* waves. Almost all the travel time data came from the Observation Reports published by the Yunnan and Sichuan seismic networks, but some arrival times were directly picked from seismograms in order to obtain a good ray coverage over the whole southwestern China. The nominal reading errors of arrival time data are 0.1 s for the first *P* and 0.2 s for *S* based on error analysis of large quantity of data.

[14] In the basic data set, the *P* arrival times data split into two branches ($\overline{P}$ and *Pn*) beyond 220 km. The width of each branch is about 8 s. However, the *S* wave data show no such branches (Figure 7). About 50% of the total first *P* arrival data is *Pn* phase. In southwestern China, nearly all earthquakes occur in the crust, so the *Pn* arrival data are indispensable for understanding the velocity structure of the uppermost mantle. Although the second *P* arrival data beyond 220 km also contain information about the crustal velocity structure, they are not utilized in our inversion.

3.3. Model Parameterization

[15] The initial model used in this paper is a 3-D model, which contains the Conrad and Moho discontinuities whose topographies are shown in Figure 4. Both deep seismic sounding profiles and the Bouguer gravity anomaly data are used to construct the initial model. The velocity values at

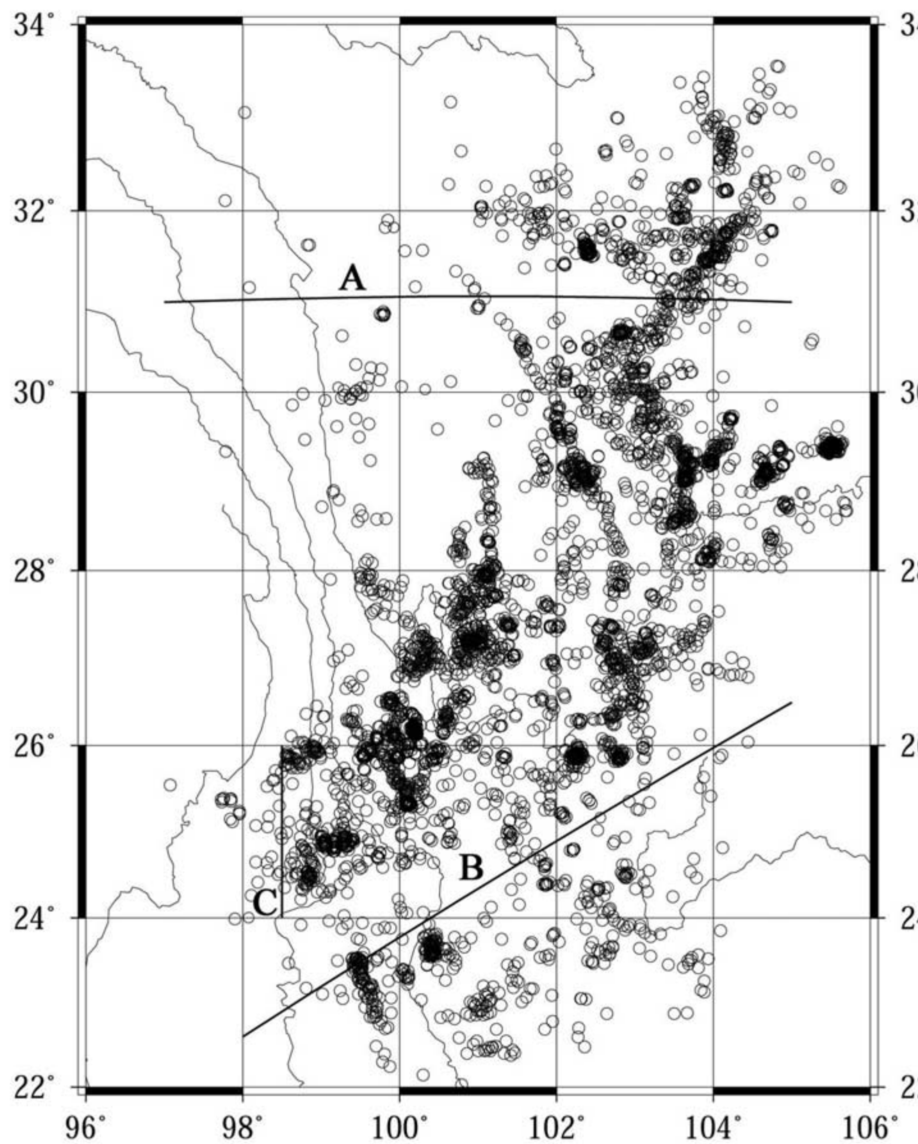

Figure 6. Epicenter distribution of the events used in the 3-D inversion of crust and upper mantle in southwestern China. Three lines (A, B, C) are the locations of cross section in 3-D velocity structure.

each layer as shown in Figure 8 and listed in Table 1 are derived from the integral interpretation of all the deep seismic sounding profiles shown in Figure 4 and the information presented by the travel time data in Figure 7. The velocity distribution in the upper, lower crust and upper mantle are uniform for the *P* and *S* phases.

[16] Among several techniques of 3-D velocity model parameterization, the grid method [*Thurber*, 1983] is the one most often used. Its advantage is that the grid net can partition the earth model at variable intervals according to the density of event epicenters and stations, to keep the sufficient ray coverage for each grid and to reduce the effect of a priori assumptions, which is necessary for rectangle block model, on the final results. In this paper, we adopt a 3-D grid model with Conrad and Moho discontinuities, where the velocity is represented as linearly continuous function except at the discontinuities. The unknowns are the velocity values at the grid nodes. The final velocity at any point in 3-D model is calculated with a linear interpolation function [*Zhao et al.*, 1992]:

$$V_m(\phi, \lambda, h) = \sum_{i=1}^{2}\sum_{j=1}^{2}\sum_{k=1}^{2} V_m(\phi_i, \lambda_j, h_k)\left[\left(1-\left|\frac{\phi-\phi_i}{\phi_2-\phi_1}\right|\right)\cdot\left(1-\left|\frac{\lambda-\lambda_j}{\lambda_2-\lambda_1}\right|\right)\left(1-\left|\frac{h-h_k}{h_2-h_1}\right|\right)\right],$$

where the subscript m indicates that the point is in the mth layer, φ is latitude, λ is longitude, h is the depth from the Earth's surface, φ_i, λ_j, h_k are the coordinates of the eight nodes surrounding the point (φ, λ, h), and $V_m(\varphi_i, \lambda_j, h_k)$ is the velocity at grid nodes in grid net of the mth layer.

[17] The geographical range of the study area is from 21° to 34°N in latitude and from 97° to 105°E in longitude. All of the node intervals in latitude and longitude are 0.5° except the boundary of the study area where the interval is

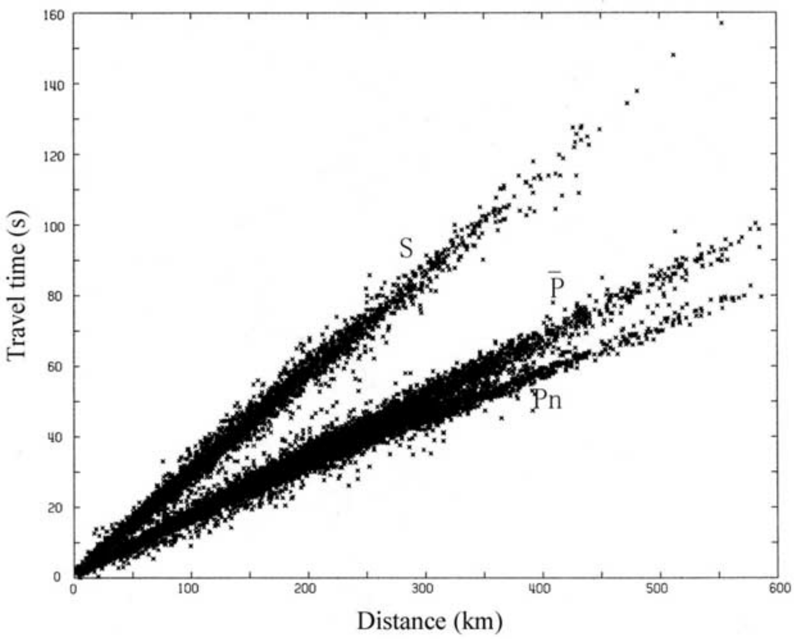

Figure 7. Travel times of *P* and *S* waves collected in Yunnan area.

1.0° (Figure 5), and the vertical grid is listed in Table 1. Total number of nodes is 2550.

3.4. Resolution Analysis

[18] The number of rays passing through each node can be used to estimate the solution's reliability. For *P* wave, among the total number of 2550 nodes, 2316 nodes have enough number of rays ($\geq$10) that enter into inversion, 1209 nodes have number of rays greater than 100, and 691 nodes greater than 500. For *S* wave, among the total number of 2550 nodes, 1222 nodes have enough number of rays ($\geq$10) that enter into inversion, 830 nodes have number of rays greater than 100, and 438 nodes greater than 500.

[19] In order to estimate the resolution, *Humphreys and Clayton* [1988] presented the Impulse Test method, which uses synthetic data to obtain the resolution matrix's column vector, so as to test the distortion effect of the equation's ill condition upon the solution. However, the resolution can only be estimated at a single node. The method is not capable of assessing the reliability of the whole solution. The checkerboard method [*Inoue et al.*, 1990] solved this problem. It extends the Impulse Test method to the whole model space, which is the superimposition of the Impulse Test for each parameter. The basic procedure of the checkerboard method is that the observation data set is replaced by a synthetic data set that is calculated from a special 3-D grid velocity model. The velocity model (i.e., checkerboard) is formed by adding perturbations with a regular distribution (i.e., the perturbation at each node has the same absolute value and is distributed in the sequence in positive and negative check) to the initial one-dimensional (1-D) velocity structure (Figure 8). Then the synthetic data set is inverted and the solution reliability is assessed by comparing the inversion result to the "checkerboard." The regular perturbation value is ±3% in this study.

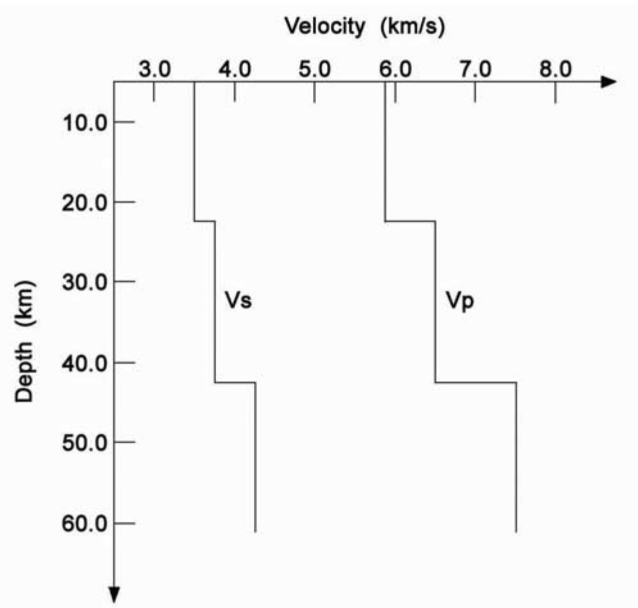

Figure 8. The 1-D initial model of velocity structure in southwestern China.

Table 1. Average Velocity at Grid Depth in Final Model and Comparison With Initial Model

	Initial			Final		
Depth, km	Vp, km/s	Vs, km/s	Vp/Vs	Vp, km/s	Vs, km/s	Vp/Vs
1	5.90	3.41	1.73	5.89	3.45	1.71
10	5.90	3.41	1.73	5.88	3.43	1.72
30	6.55	3.78	1.73	6.45	3.74	1.72
50	7.77	4.36	1.78	7.75	4.35	1.78
65	7.82	4.39	1.78	7.80	4.35	1.79
85	7.88	4.41	1.78	8.00	4.42	1.81

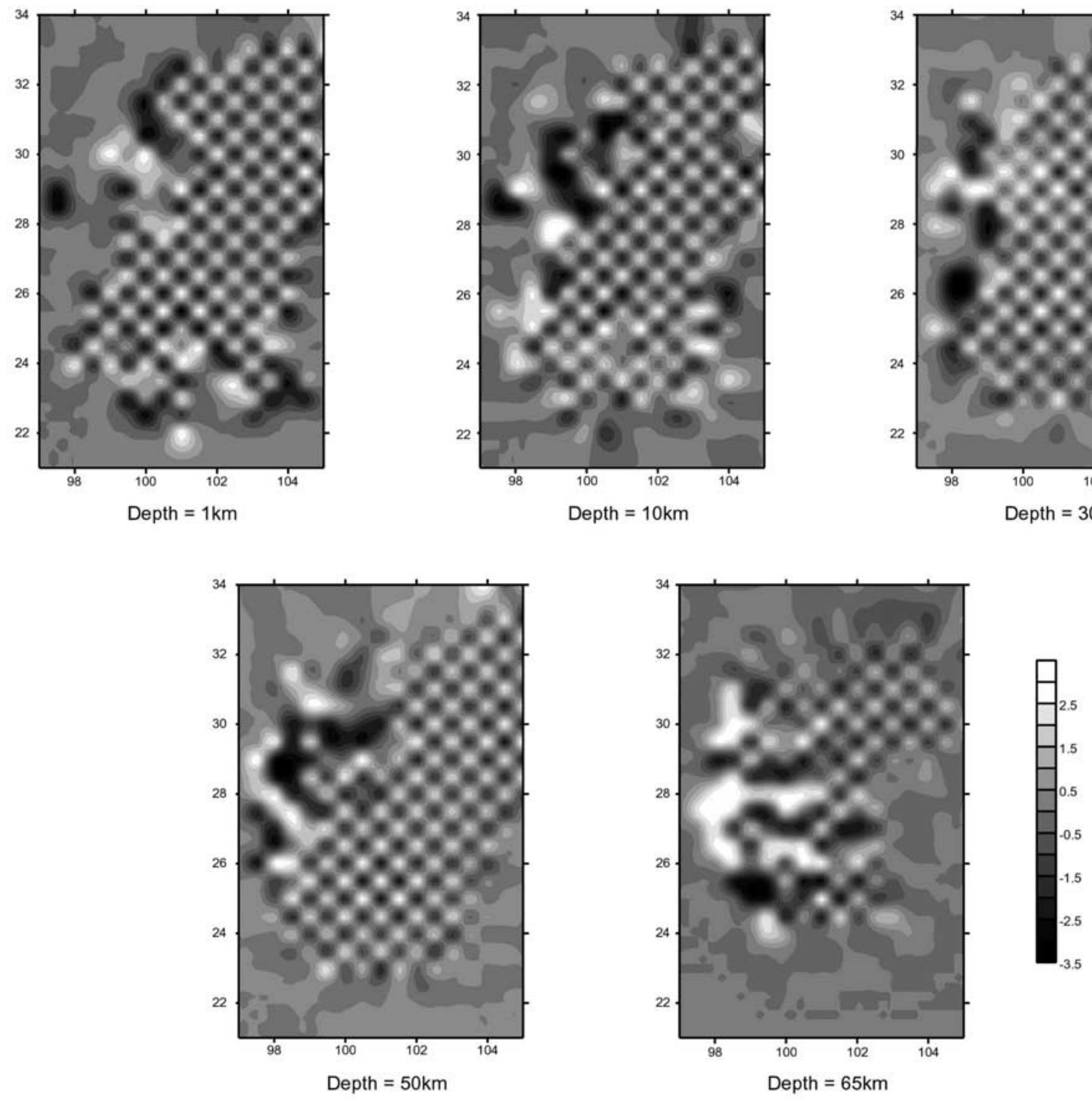

Figure 9. Checkerboard resolution test result for *P* wave velocity.

[20] Application of the checkerboard method to *P* wave and *S* wave data, respectively, reveals that the resolution is satisfactory for most nodes at various depths. For example, for *P* wave velocity (Figure 9), the resolution in northwestern region (west of 100.5° and north of 28°) is lower at depth of 10 km because the region has small number of stations and earthquake events. The extent for which resolution is poor in the western region at depth of 30 km is smaller than at depth of 10 km. However, in the greater part of the study region, where it can be resolved, the resolution is relatively poor because of lack of data for *P** phase (refracted from Conrad) arrival times. Enough *Pn* phase arrival time data have been used in this study, and so, except for the northwest region, the resolution is high at depth of 50 km, which is comparable with the resolution in the upper crust.

4. Velocity Models

[21] The inversion of the *P* wave velocity structure model requires five iterations. The inversion method stops when the RMS travel time residual no longer continues to reduce. The initial travel time residual sum of squares is 57,847.60, and the RMS residual is 0.92 s, and the travel time residual sum of squares reduces to 21304.78, and the RMS residual reduces to 0.57 s after 5 iterations. The inversion of *S* wave velocity structure model requires four iterations. The initial travel time residual sum of squares is 69,843.05 and the RMS residual is 1.13 s, and the travel time residual sum of squares reduces to 24565.82 and the RMS residual reduces to 0.72 s after four iterations. Considering that the networks in this region have been operated for a long time, with several types of instruments, and repeated instrument change, this error assessment is acceptable. Figures 10 and 11 show the results of the inversions for *P* wave and *S* wave velocity structure in southwestern China. Table 1 shows the velocity of each node at different depths after inversion. It is the initial value plus the average of anomalies of each node at the same depth. The velocity anomaly distributions at depths of 10 km, 30 km and 50 km indicate the characteristics of lateral variation of velocity in the

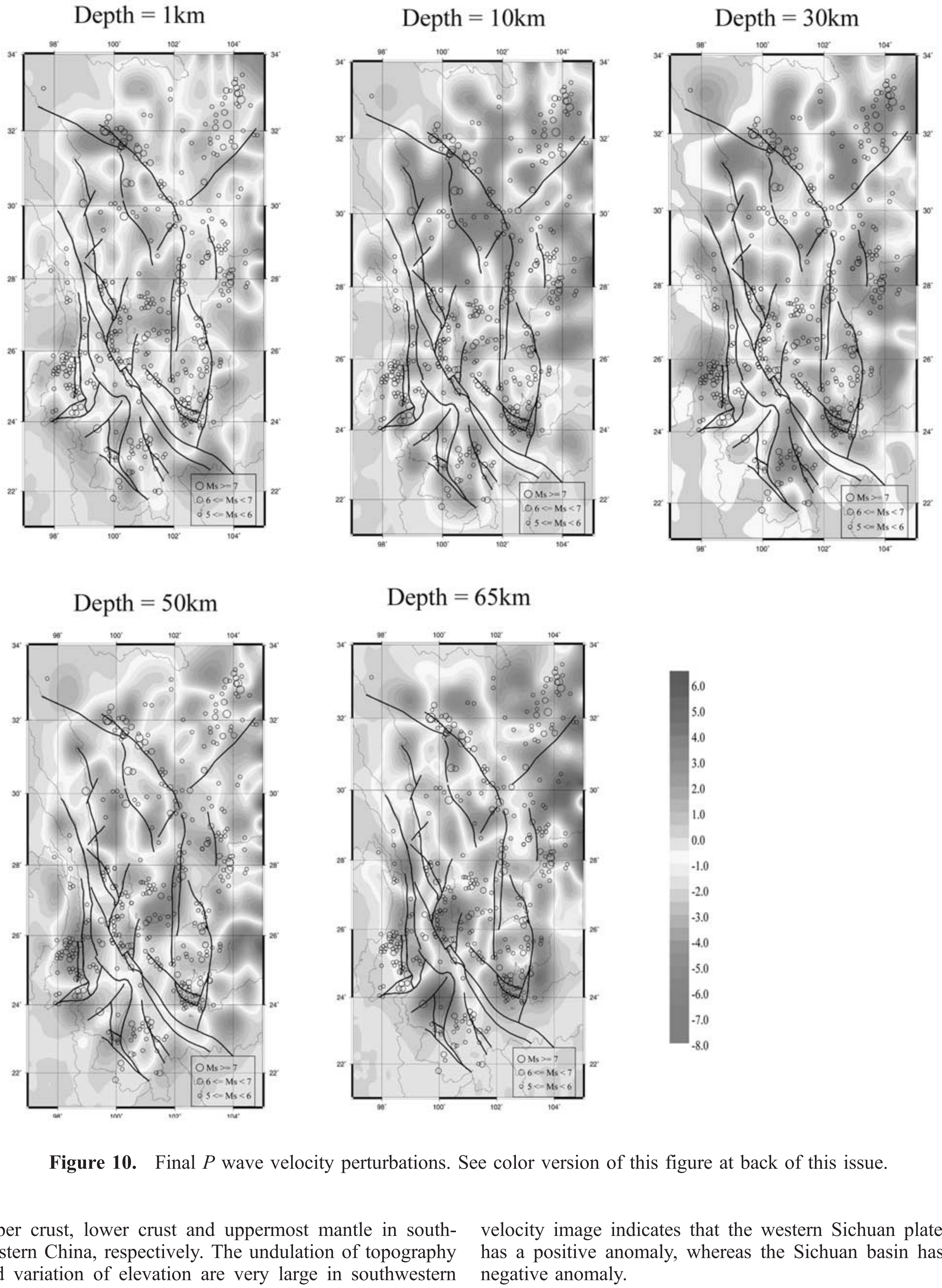

Figure 10. Final P wave velocity perturbations. See color version of this figure at back of this issue.

upper crust, lower crust and uppermost mantle in southwestern China, respectively. The undulation of topography and variation of elevation are very large in southwestern China. Both the western Sichuan Plateau and the Sichuan Basin are negative P wave velocity anomaly regions at depth of 1 km, perhaps related to higher elevation, or to low-velocity sedimentary layers. However, the S wave velocity image indicates that the western Sichuan plateau has a positive anomaly, whereas the Sichuan basin has a negative anomaly.

4.1. Upper Crust

[22] The velocity anomaly distribution at 10 km depth is clearly related to the surface tectonics. The Sichuan Basin

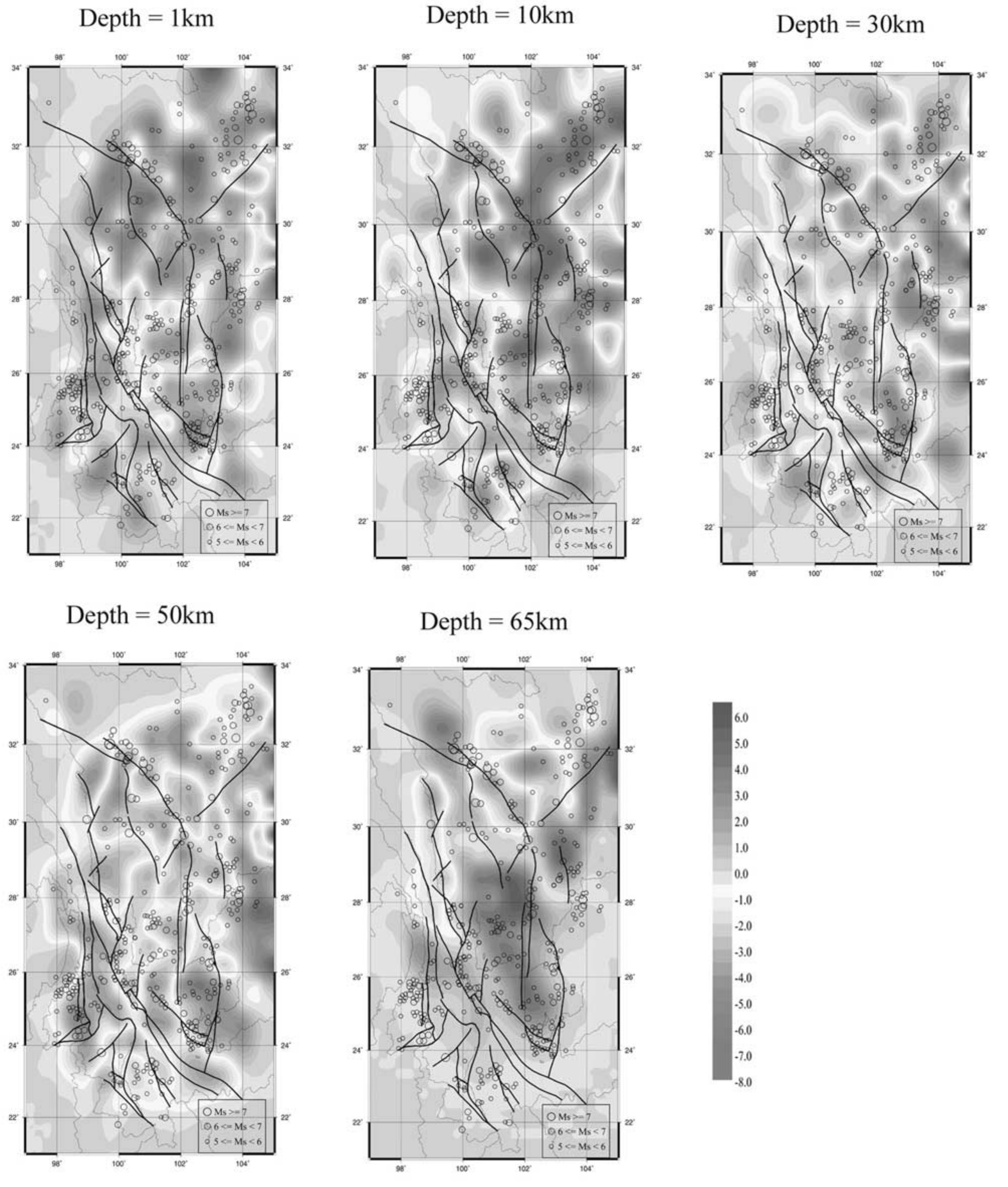

Figure 11. Final *S* wave velocity perturbations. See color version of this figure at back of this issue.

(east of 103.5°E and 29°∼31°N) is associated with a negative anomaly at depth of 1 km and a positive velocity anomaly at depth of 10 km. This suggests the presence of a low-velocity sedimentary layer of large thickness. A negative velocity anomaly region of large extent exists in the upper crust of western Sichuan, consistent with the velocity structure of southern Tibetan plateau [*Kind et al.*, 1996]. The Longmenshan Fault zone is located at the boundary between a positive anomaly (west flank) and a negative anomaly (east flank). However, in the south segment of the fault, the west flank is the Chengdu-Ya'an local negative anomaly zone, and the east flank is the Qionglaishan local positive anomaly zone. Although different from the north segment of the fault, this is consistent with the free-air gravity anomaly (Figure 3b). Additionally, in some negative velocity anomaly regions related to regional strike-slip fault, such as the south segment of the Xianshuihe Fault and the north segment of the Anninghe Fault, strong earthquakes have rarely occurred during recent times. Furthermore, the Tengchong area is also a negative anomaly region that is likely related to geothermal activity. In the region south of 28°N, except for the Tengchong area, the velocity anomalies are relatively small, whereas the Chuxing area and the area south of Simao appear to be negative anomaly regions.

[23] As for the *S* wave velocity anomaly, the region from west flank of the Longmenshan Fault to the north flank of the Anninghe Fault appears to be a positive velocity anomaly belt. However, a reasonable interpretation related to deep layers has not been obtained.

4.2. Lower Crust

[24] Considering the *P* wave velocity anomaly at depth of 30 km, the western Sichuan plateau and the region east of the Anninghe Fault show negative anomalies. The main seismic belts in southwestern China, such as the Anninghe belt, the Xianshuihe belt, the Songpan-Pingwu belt, the Xiaojiang belt, the Red River belt and the Mabian belt, all show negative anomaly. However, the Lancang-Gengma belt and the Tengchong-Longling belt do not show negative anomalies; an exception is the Tengchong area with a positive anomaly.

[25] Similar to the upper crust, the Longmenshan Fault is located at the boundary between positive and negative anomalies. The Red River Fault is a transition zone from positive anomaly to negativity anomaly, whereas the area south of the fault clearly shows a negativity anomaly and the area north of the fault is mostly positive anomaly region. This negative anomaly makes the mean crustal velocity lower than that in the region south of the fault. These results are consistent with interpretation of deep seismic sounding profiles [*Hu et al.*, 1986].

[26] The *S* wave velocity anomaly distribution in the lower crust has features similar to the *P* wave anomalies. For example, the Sichuan Basin has a positive anomaly and several main seismic belts show a negative anomaly.

4.3. Upper Mantle

[27] In the velocity anomaly at depth of 50 km, the Panxi tectonic zone and the Tengchong volcano geothermal region are large-scale negative anomaly regions. The negative anomaly in Panxi area is consistent with the results of deep seismic profiles [*Xiong et al.*, 1986]. In addition, the velocity anomaly image is clearly partitioned by some large faults with definite association to the crustal and upper mantle features. For example, the Longmenshan Fault lies at the boundary between a positive anomaly and a negative anomaly. The Xianshuihe Fault, the Xiaojiang Fault and the Red River Fault are in the region of negative anomaly, although their anomaly values are smaller than those of the Panxi tectonic zone and the Tengchong volcanic geothermal region. In some seismic belts, the uppermost mantle appears as a *P* wave negative anomaly region, similar to the lower crust. The velocity anomaly at depth of 65 km clearly shows the velocity anomaly feature of the upper mantle in northwest region of the study region. Because most earthquakes occur in the middle to upper crust in southwestern China, the arrival time data set does not offer much information on lateral variation of velocity structure at depth of 85 km in this study.

[28] The *S* wave velocity anomaly distribution at depth of 50 km shows features similar to those for *P* wave. For instance, some seismic belts show negative anomalies. In addition, it shows a negative anomaly in the southwestern Yunnan region (including the Tengchong area). As mentioned above, the *S* wave travel time has features different than those of the *P* wave travel time in Figure 7, where the branch beyond the relevant distance (220 km) is not clearly defined. Therefore the *S* wave anomaly at depth of 65 km has low reliability.

[29] The results of deep seismic sounding [*Kan et al.*, 1986] indicate that there is no clear evidence of a sharp velocity change across the Red River Fault. This is inconsistent with the image obtained in this paper. The reason probably is that the deep seismic profiles only cross over the north segment of the Red River Fault (near the city of Dali), where there are several intersecting faults and the geologic setting is complicated. Nevertheless, the seismic rays corresponding to large amounts of travel time date used in this paper have provided good coverage for the entire Red River Fault.

5. Discussion and Conclusions

[30] The 3-D velocity models of the crust and upper mantle in southwestern China reveal many significant characteristics that are basically consistent with the results of deep seismic sounding. For example, there is the velocity difference in the lower crust across the Red River Fault [*Hu et al.*, 1986]; a low velocity zone exists in the middle crust and the upper mantle in the Panxi tectonic zone [*Xiong et al.*, 1986]; and a lower velocity in the upper mantle exists in the Longmenshan tectonic belt [*Chen et al.*, 1988]. We will discuss below global features of crustal and upper mantle structure, velocity anomalies related to faults, velocity anomaly features in the Tenchong volcano geothermal region and seismotectonics of the region.

5.1. Global Features of Crustal and Upper Mantle Structure in Southwestern China

[31] Southwestern China is a region of strong earthquake activity. The results in this study and other research on deep crustal structure reveal that southwestern China is a tectonically active region. As mentioned before, the crustal thickness varies by about 30 km in this region. Variation of crustal thickness is generally related to many kinds of tectonic activity, for instance, extension and compression of crust, isostasy, underplating and intrusion of magma, etc. The main tectonic activity in southwestern China is the subduction and indentation of the Indian plate. There are high heat flow values in west Yunnan and Panxi areas [*Wu et al.*, 1988]. The high heat flow is generally related to tectonic activity (magmatism). In addition, high-conductivity layers exist in the crust and/ or upper mantle of western Yunnan and western Sichuan.

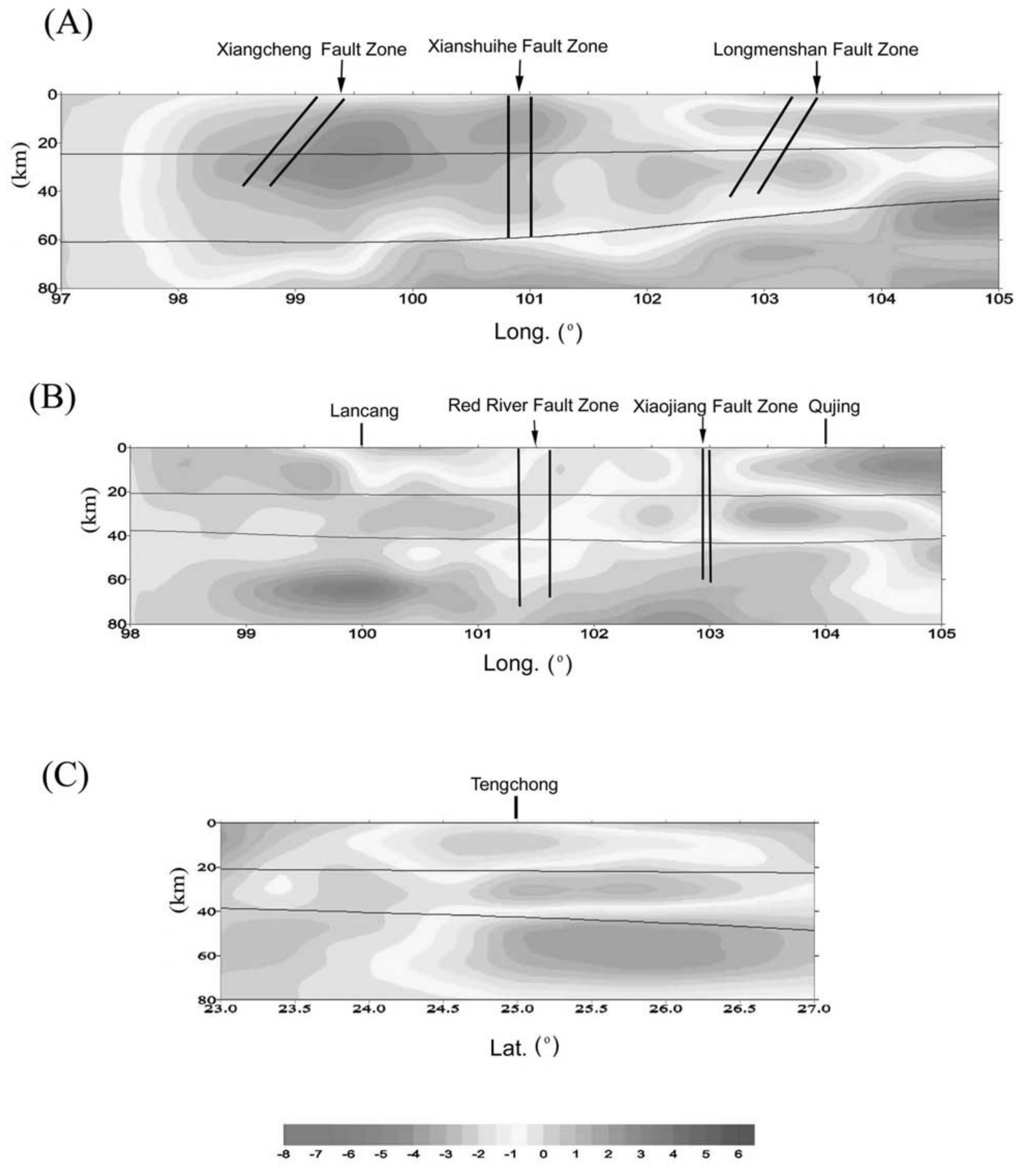

Figure 12. (a) *P* velocity structure of the cross section A across Xianshuihe Fault and Longmenshan Fault. (b) *P* velocity structure of the cross section B across Red River Fault and Xiaojiang Fault. (c) *P* velocity structure of the cross section C in Tengchong volcanogeothermal region. The location of A, B, and C are shown in Figure 6. See color version of this figure at back of this issue.

It is considered that the high-conductivity layers are related to partial melt or detachment [*Sun et al.*, 1989; *Li and Jin*, 1988].

[32] The mean crustal velocity of 6.25 km/s in southwestern China is lower than the global mean crustal velocity in continents. Meanwhile, there is a large-scale negative velocity anomaly in the lower crust. All these accord with the known features of tectonic activity [*Mooney and Brocher*, 1987]. The low-velocity anomaly at 10 km depth in western Sichuan is consistent with the eastern Tibetan plateau. In

addition, the average velocity of uppermost mantle in southwestern China is 7.75 km/s, obviously lower than the global mean velocity of *Pn* (8.1 km/s) in continents. The low mean Pn velocity is probably related to the dominance of thermal processes throughout the Cenozoic [*Mooney and Braile*, 1989]. Magmatic underplating may generate both an anomalous low velocity zone in the lower crust and a diffuse Moho discontinuity. At the same time, a negative velocity anomaly in the uppermost mantle weakens the energy reflected from the Moho. This appearance was observed in the deep seismic sounding profiles in southwestern China [*Kan et al.*, 1986].

5.2. Velocity Anomalies Related to Faults

[33] Anomalies under major fault belts in southwestern China extend down to the uppermost mantle in the 3-D velocity results. The Longmenshan Fault belt is a thrust fault. In the velocity anomaly distribution, it is located in the transition zone between positive and negative anomalies. The *P* velocity at depth of 10 km has a positive anomaly in the east and negative in the west. The *P* velocity anomaly at depths of 30 km and 50 km are similar to that at depth of 10 km, while the anomaly boundary has slightly moved to the west at depth of 50 km (Figure 12a).

[34] The Xianshuihe Fault is one of the most active strike-slip faults in China in recent 100 years. The negative anomaly exists along the fault, at depth of 30 km and 50 km (Figure 12a). The Anninghe Fault, the Xiaojiang Fault and the Red River Fault are also strike-slip faults. Some of these are also located in the negative anomaly area, but their anomaly values are lower than that of the Xianshuihe Fault (Figure 12b). Other faults are located in the transition zone between positive and negative anomalies. Although the resolution of the northwestern portion of study area is lower in the 3-D velocity structure inversion, the anomaly of the Jinshajiang Fault belt appears in the upper mantle.

[35] Being affected by plate collision, southwestern China obviously shows complex deformation and movement, such as crustal thickening and shortening, plateau uplift, block rotation, lateral extrusion, and other features. Although local negative anomalies are found in the crust and uppermost mantle in the Sichuan-Yunnan Rhombic Block, it shows relatively high velocity on the whole. The strike-slip faults around the block (such as the Xianshuihe Fault, the Xiaojiang Fault and the Red River Fault) present negative anomaly down to the upper mantle, which is conducive to the lateral extrusion of crustal blocks along the faults.

5.3. Features of Velocity Anomaly in Tengchong Geothermal Region

[36] A prominent feature in the Tengchong region is the negative anomaly in the uppermost mantle. Figure 12c shows a cross section of two-dimensional velocity structure, produced from the 3-D velocity anomaly obtained in this study, along south-north direction and passing through the Tengchong geothermal region. The segment from Zhongshan to ZiZhi in Figure 12c coincides with a deep seismic sounding profile [*Wang et al.*, 2002]. Figure 12c indicates that the upper crust and upper mantle show negative anomalies, while the lower crust shows positive anomaly. This is consistent with the model produced from deep seismic sounding. Other research indicates that there is lower resistivity in the crust, high heat flow, and low *Q* value in this region [*Sun et al.*, 1989; *Wu et al.*, 1988; *Qin et al.*, 1998]. Therefore it is inferred that the upper crust contains hot material related to magma, which comes from upper mantle, and passes through thin channels in the lower crust (e.g., near vertical fault). The negative velocity anomaly in the upper crust is probably related to the magmatic differentiation.

5.4. Seismotectonics

[37] In southwestern China, strong earthquakes are located along the following seismic belts: Longmenshan belt, Xiaoshuihe belt, Anninghe belt, Mabian belt, Xiaojiang belt, Red River belt, Lancang-Gengma belt, and Tengchong-Longling belt. *Fan* [1978] suggested that most earthquakes are distributed along fault belts that have been active since the Tertiary period. These fault belts outline irregular blocks involved in regional seismic activity. The Xiaoshuihe belt, Anninghe belt, Xiaojiang belt, and Red River belt lie on the frame of the Rhombic Block. Most strong earthquakes in southwestern China are found to be inside the block or on its boundary.

[38] As mentioned above, most large faults in southwestern China are closely related to modern strong seismogenic zones. The modern seismotectonic zones in this region are mainly under a regional stress field with compression in nearly north-south direction, despite the existence of some local stress fields with compression in the east-west direction [*Kan et al.*, 1977].

[39] The focal depths of most earthquakes in southwestern China are between 5 km and 25 km, which is the range of upper to middle crust, where the crustal medium is brittle. The velocity anomaly images in this depth region reveal that most strong earthquakes are located in the transition zone between positive and negative anomalies (Figure 10). The negative velocity anomaly exists beneath the hypocenters of these earthquakes with depth (lower crust, sometimes including the upper mantle) (Figures 10 and 11). In short, the deep crustal environment of most strong earthquakes in southwestern China is associated with normal velocity or positive velocity anomaly in the focus area and negative velocity anomaly beneath the area. The negative velocity anomaly in the lower crust and uppermost mantle beneath the Xianshuihe seismic belt is greater than those in the Anninghe Seismic belt and the Xiaojiang Seismic belt. Of course, the seismotectonics of southwestern China is very complex, and each seismic belt has its own special environment.

[40] **Acknowledgments.** The research of C.-Y. Wang is supported jointly by the State Key Basic Research Development and Programming Project (G1998040700) and the Climb Program (95-S-05-01) of National Scientific and Technological Ministry of China. The work of W. W. Chan is supported by Small Business Innovative Research Grant DE-FG02-99-ER82837. The Yunnan and the Sichuan Seismic Network helped us in collecting the basic seismic data. Sincere thanks are due D. P. Zhao, who provided his tomographic inversion code and generous help with the calculations.

References

Aki, K., and W. H. K. Lee, Determination of three-dimensional velocity anomalies under a seismic array using *P* arrival times from local earthquakes: 1. A homogeneous initial model, *J. Geophys. Res.*, *81*, 4381–4399, 1976.

Allen, C. R., A. R. Gillespie, and Y. Han, Red River and associated faults, Yunnan Province, China: Quaternary geology, slip rates, and seismic hazard, *Geol. Soc. Am. Bull.*, *95*, 686–700, 1984.

Allen, C. R., Z. Luo, and H. Qian, Field study of a high active fault zone: The Xianshuihe fault of southwestern China, *Geol. Soc. Am. Bull.*, *103*, 1178–1190, 1991.
Chen, B. W., K. W. Wang, and W. X. Liu, Geotectonics in Nujiang--Lancangjiang-Jinshajiang Region (in Chinese), 204 pp., Geol. Publ., Beijing, 1987.
Chen, P. S., F. T. Liu, and Q. Li, Lateral inhomogeneity of velocity structure in Yunnan region (in Chinese), *Sci. China, Ser. B*, *4*, 431–438, 1990.
Chen, X. B., Y. Q. Wu, and P. S. Du, Crustal velocity structure at the two flanks of Longmenshan tectonic belt (in Chinese), in *Developments in the Research of Deep Structures of China's Continent*, edited by Dep. of Sci. Programm. and Earthquake Monit., pp. 112–127, Geol. Press, Beijing, 1986.
Chen, X. B., Z. Y. Lin, N. Y. Wu, Upper mantle with lower velocity in eastern margin of Tibetan plateau (in Chinese), in *Selection of Papers on Crustal Structure and Stress*, vol. 2, pp. 159–166, Seismol. Press, Beijing, 1988.
Cui, Z. Z., J. P. Chan, and L. Wu, *Huashixia-Shaoyang Deep Crustal Structure and Tectonics* (in Chinese), pp. 156–168, Geol. Publ., Beijing, 1996.
Fan, P., Outline of the tectonic evolution of southwestern China, *Tectonophysics*, *45*, 261–267, 1978.
Hu, H., H. Lu, and C. Wang, Explosion investigation of the crustal structure in western Yunnan Province (in Chinese), *Acta Geophys. Sin.*, *29*(2), 144–154, 1986.
Humphreys, E., and R. W. Clayton, Adaptation of back projection tomography to seismic travel time problems, *J. Geophys. Res.*, *93*, 1073–1085, 1988.
Inoue, H., Y. Fukao, K. Tanabe, and Y. Ogata, Whole mantle *P*-wave travel time tomography, *Phys. Earth Planet. Inter.*, *59*, 294–328, 1990.
Jiang, C. S., Volcanoes and earthquakes in Tengchong area, Yunnan Province, China, *J. Seismol. Res.*, *8*, 107–120, 1985.
Kan, R. J., S. C. Zhang, and F. T. Yan, Modern tectonic stress field in southwestern China(in Chinese), *Acta Geophys. Sin.*, *20*(2), 96–110, 1977.
Kan, R. J., H. X. Hu, R. S. Zeng, W. D. Mooney, and T. V. McEvilly, Crustal structure of Yunnan Province, People's Republic of China, from seismic refraction profiles, *Science*, *234*, 433–437, 1986.
Kind, R., J. Ni, and W. Zhao, Evidence from earthquake data for a partially molten crustal layer in southern Tibet, *Science*, *274*, 1692–1694, 1996.
Leloup, P., R. Lacassin, and P. Tapponnier, The Ailao Shan-Red River shear zone (Yunnan, China), Tertiary transform boundary of Indochina, *Tectonophysics*, *251*, 73–84, 1995.
Li, L., and G. Y. Jin, Lithospheric electricity structure in Panxi region (in Chinese), in *Selection of Papers on the Panxi Rift*, vol. 3, pp. 66–75, Geol. Press, Beijing, 1988.
Li, P., *Xianshuihe-Xiaojiang Fault Belt* (in Chinese), 50 pp., Seismol. Press, Beijing, 1993.
Lin, Z., H. Hu, and W. Zhang, The preliminary interpretation of deep seismic sounding in western Yunnan (in Chinese), *Acta Seismol. Sin.*, *15*(4), 282–295, 1993.
Liu, J. H., F. T. Liu, and H. Wu, Three dimensional velocity structure of crust and upper mantle in South-North Zone of China (in Chinese), *Acta Geophys. Sin.*, *32*(2), 143–151, 1989.
Mooney, W. D., and L. W. Braile, The seismic structure of the continental crust and upper mantle of North American, in *The Geology of North America*, vol. A, *The Geology of North America—An Overview*, edited by A. W. Bally and A. R. Palmer, pp. 39–52, Geol. Soc. of Am., Boulder, Colo., 1989.
Mooney, W. D., and T. M. Brocher, Coincident seismic reflection/refraction studies of the continental lithosphere: A global review, *Rev. Geophys.*, *25*, 723–742, 1987.
Qin, J. Z., G. Huangfu, and J. W. Zhang, Characteristics of Q values around Tengchong volcano and adjacent areas (in Chinese), *J. Seismol. Res.*, *21*, 358–361, 1998.
Ren, J. S., C. F. Jiang, and Z. K. Zhang, *Tectonics in China and Its Evolution* (in Chinese), 124 pp., Science Press, Beijing, 1980.
Sun, J., C. F. Xu, and Z. Jiang, Electricity structure of crust and upper mantle in western Yunnan and its relation to crustal activity (in Chinese), *Seismol. Geol.*, *11*(1), 35–45, 1989.
Tapponnier, P., R. Lacassin, and P. H. Leloup, The Ailao Shan/Red River metamorphic belt: Tertiary left-lateral shear between Indochina and South China, *Nature*, *343*, 431–437, 1990.
Thurber, C. H., Earthquake locations and three-dimensional crustal structure in the Coyote lake area, central California, *J. Geophys. Res.*, *88*, 8226–8236, 1983.
Wang, C. Y., X. L. Wang, and Q. Z. Yan, Three dimensional velocity structure beneath Kunming Seismic Network (in Chinese), *Acta Seismol. Sin.*, *16*(2), 167–175, 1994.
Wang, C. Y., H. Lou, J. P. Wu, Z. M. Bai, G. Huangfu, and J. Z. Qin, Seismological study on the crustal structure of Tengchong volcano-geothermal area, *Acta Seismol. Sin.*, *15*(3), 247–259, 2002.
Wu, Q. F., J. H. Zu, and Y. Z. Xie, Basic geothermal characteristics in Yunnan Province (in Chinese), *Seismol. Geol.*, *10*(4), 177–183, 1988.
Xiong, S. B., J. W. Teng, and Z. X. Yin, Explosive seismological investigation of crustal and upper mantle structure in southern Panxi tectonic zone (in Chinese), *Acta Geophys. Sin.*, *29*(3), 235–244, 1986.
Yan, Q. Z., G. Q. Zhang, H. X. Hu, and R. J. Kan, Crustal structure along Simao-Malong profile in Yunan Province, *Seismol. Res.*, *8*, 249–280, 1985.
Zhao, D., A Tomographic study of seismic velocity structure in the Japan Islands, Ph.D. thesis, 301 pp., Tohoku Univ., Sendai, 1991.
Zhao, D., A. Hasegawa, and S. Horiuchi, Tomographic imaging of *P* and *S* wave velocity structure beneath northeastern Japan, *J. Geophys. Res.*, *97*, 19,909–19,928, 1992.

W. W. Chan, Multimax, Inc., 1441 McCormick Drive, Largo, Maryland 20774, USA. (winston@multimax.com)
W. D. Mooney, U.S. Geological Survey, Menlo Park, California, USA.
C.-Y. Wang, Institute of Geophysics, China Seismological Bureau, Beijing, China.

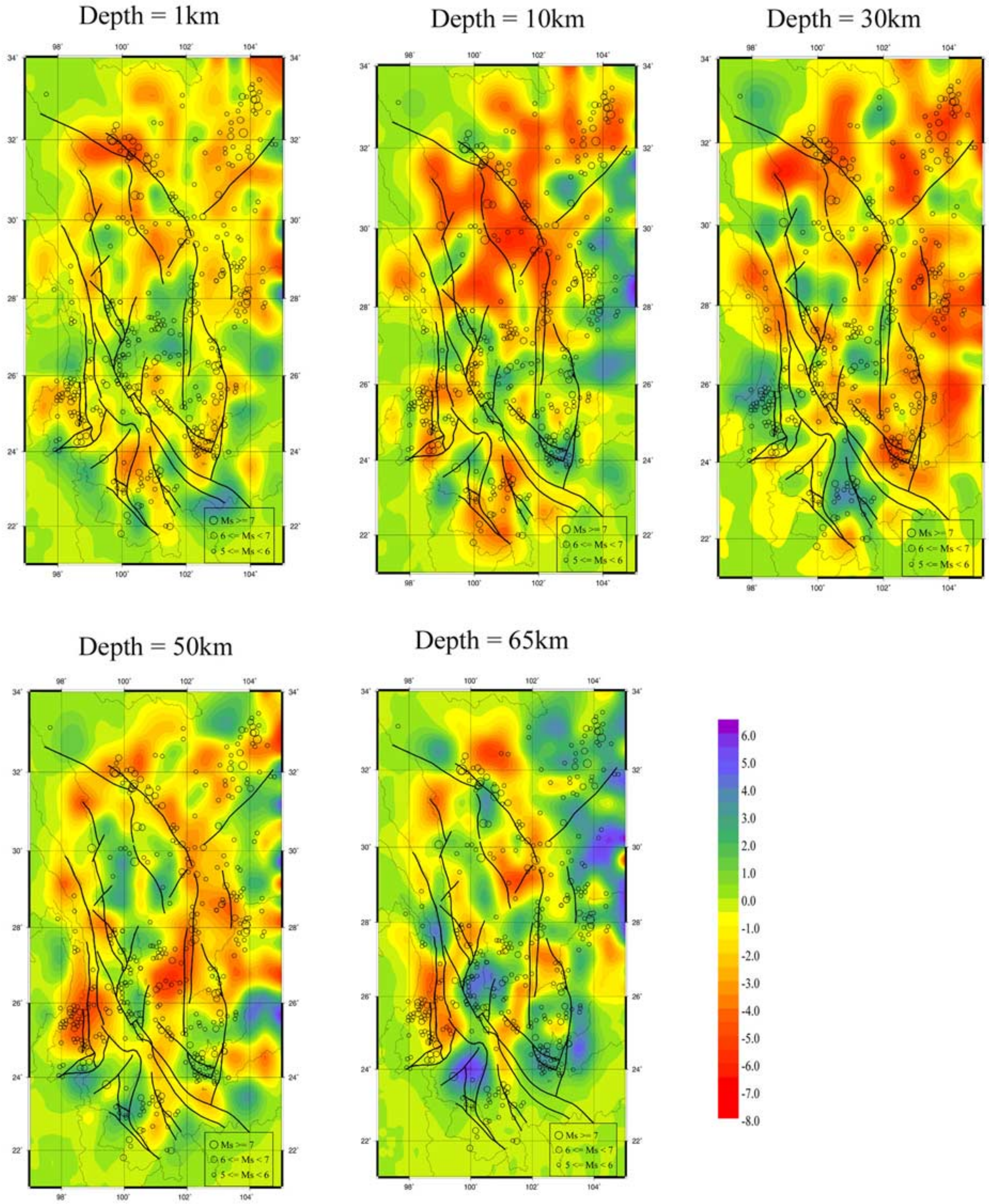

Figure 10. Final *P* wave velocity perturbations.

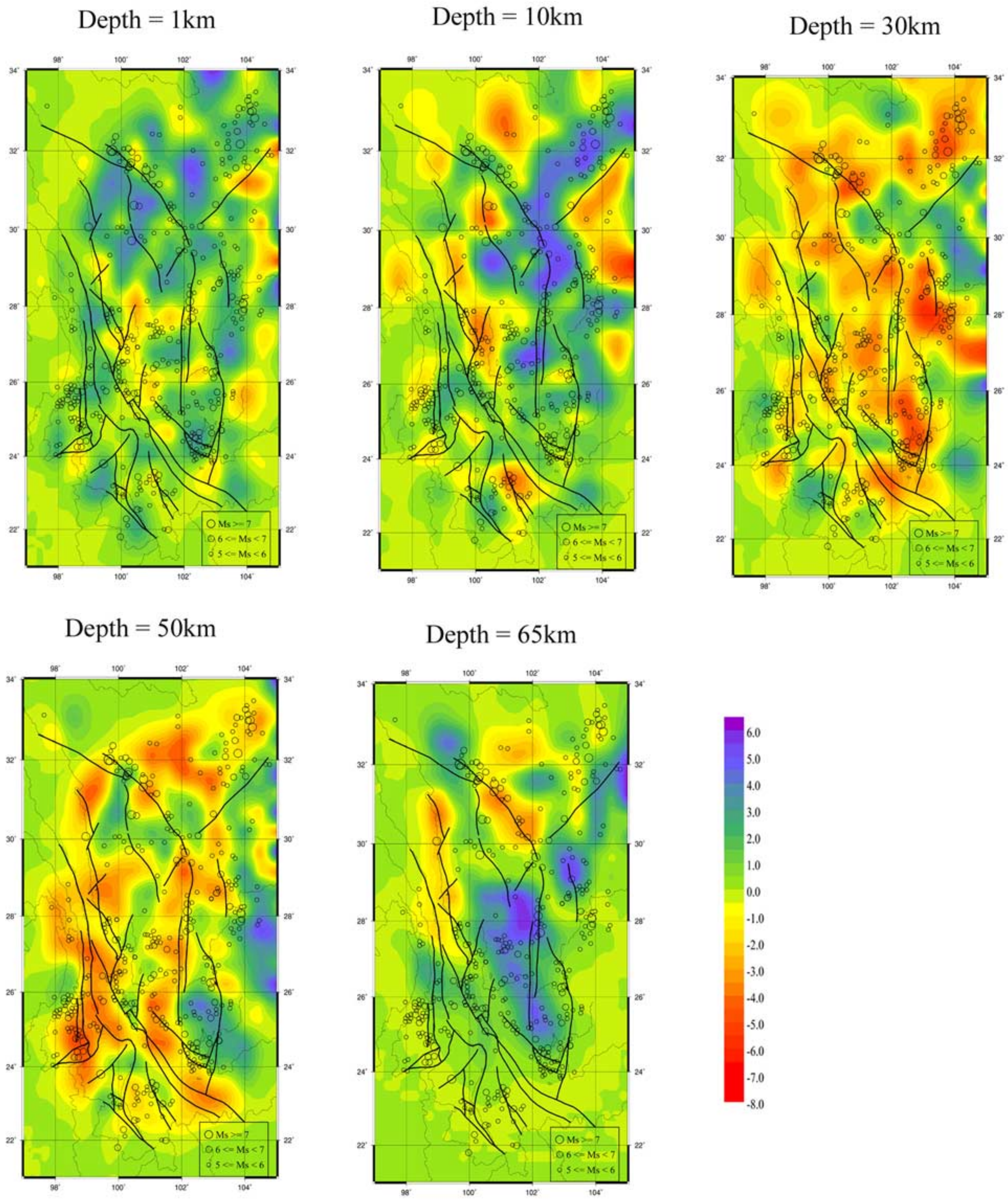

Figure 11. Final *S* wave velocity perturbations.

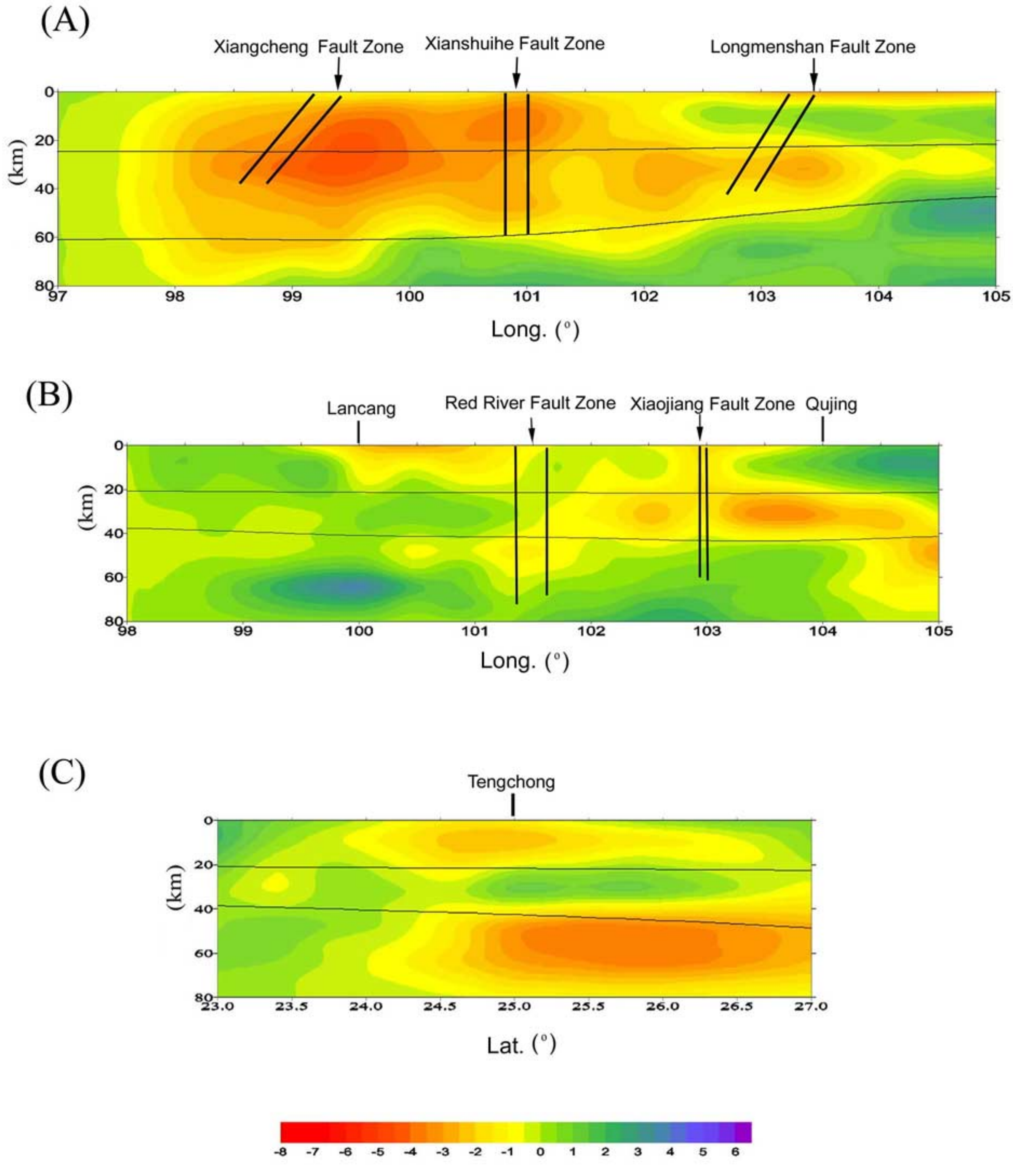

Figure 12. (a) *P* velocity structure of the cross section A across Xianshuihe Fault and Longmenshan Fault. (b) *P* velocity structure of the cross section B across Red River Fault and Xiaojiang Fault. (c) *P* velocity structure of the cross section C in Tengchong volcanogeothermal region. The location of A, B, and C are shown in Figure 6.